



# Experimental and Theoretical Investigation of Thermophysical Properties of Synthesized Hybrid Nanofluid Developed by Modeling Approaches

Fatemeh Nasirzadehroshenin<sup>1</sup> · Alireza pourmozafari<sup>1</sup> · Heydar Maddah<sup>2</sup> · Hossein Sakhaeinia<sup>3</sup>

Received: 11 August 2019 / Accepted: 14 January 2020 / Published online: 28 January 2020  
© King Fahd University of Petroleum & Minerals 2020

## Abstract

Although, titanium oxide (TiO<sub>2</sub>) has appropriate mechanical and chemical stability used in different applications, its thermal conductivity slightly increases with an increasing temperature and concentration compared with other metal oxides such as aluminum oxide (Al<sub>2</sub>O<sub>3</sub>). Thus, synthesized aluminum oxide nanoparticles were incorporated on the surfaces of titanium oxide in ultrasonication condition with purpose of thermophysical properties modification. The scanning electron microscopy and X-ray diffraction were used to investigate the structure and morphology of synthesized nanocomposite. The impact of variables (temperature, volume fraction and nanoparticle size) on the thermal conductivity and viscosity of prepared hybrid nanofluid was investigated using KD2Pro instrument and Brookfield DVII viscometer, respectively. Results showed a significant improvement of thermophysical properties of prepared hybrid nanofluid, compared to water or untreated titanium oxide–water. The results showed that three mentioned variables considerably affect the thermophysical properties of hybrid nanofluid; as an increasing volume fraction, reducing nanoparticle size and temperature led to an increasing viscosity while enhanced thermal conductivity was resulted from an increasing nanofluid volume fraction and temperature, and a decreasing nanoparticle size. This was confirmed using two computer-modeling approaches, which allow optimization of the thermophysical properties of hybrid nanofluid. Modifying Response Surface Methodology-Central Composite Design (RSM-CCD) estimated accurately the optimal conditions for thermal conductivity and viscosity. The best artificial neural network model was chosen based on its predictive accuracy for estimation of thermophysical properties; having seven neurons in hidden layer and minimum error, demonstrated the most accurate approach for modeling the considered task.

**Keywords** Nanofluids (NFs) · Nanocomposite · Response surface methodology-central composite design (RSM-CCD) · Artificial neural network (ANN) · Thermophysical properties

## List of Symbols

$T$  Temperature (°C)  
 $k$  Thermal conductivity W/m. K  
 $D$  Average crystal size (nm)

## Greek Letters

$\mu$  Dynamic viscosity (kg/mS)Pa.s  
 $\varphi$  Volume fraction %v/v  
 $\rho$  Density(kg/m<sup>3</sup>)  
 $\lambda$  Wavelength

✉ Fatemeh Nasirzadehroshenin  
Maryam.nasrzade@gmail.com;  
Fatemeh.nasirzade@student.unisi.it

<sup>1</sup> Department of Biotechnology, Chemistry and Pharmacy (DBCF), Siena University, Via A Moro, 2, 53100 Siena, Italy

<sup>2</sup> Department of Chemistry, Payame Noor University (PNU), 19395-3667, Tehran, Iran

<sup>3</sup> Department of Chemical Engineering, Central Tehran Branch, Islamic Azad University, Tehran, Iran

## 1 Introduction

A nanofluid contains solid particles in nanoscale (dimensional range of approximately 1–100 nm) dispersed in a liquid, are used to enhance thermophysical properties compared to the base fluid. The nanoparticles used in nanofluids are typically made of metals, oxides, carbides, or carbon nanotubes. Common base fluids include water, ethylene glycol and oil [1]. Novel properties of nanofluids allow them to be beneficial heat transfer fluids in many engineering



applications ranging in microelectronics, engine cooling/vehicle thermal management, fuel cells, domestic refrigerator, heat exchanger, chiller, pharmaceutical processes, etc., [2–11]. The thermal conductivity and the heat transfer increase in nanofluid compared to the base fluid [12]. Prepared hybrid (composite) nanoparticles may alter or change the thermal conductivity of nanoparticles. Composition of two or more different materials in nanoscale is defined as hybrid nanoparticles. Hybrid nanoparticles or nanocomposites are dispersed into base fluid such as water, ethylene glycol and oil to produce hybrid nanofluids. Thus, the motivation for the preparation of hybrid nanofluid is mostly associated with reaching further heat transfer enhancement due to enhanced nanofluid thermal conductivity [13, 14].

Masuda et al. [15] showed that synthesized nanofluids such as alumina ( $\text{Al}_2\text{O}_3$ )-water, titanium oxide ( $\text{TiO}_2$ )-water and silicon dioxide ( $\text{SiO}_2$ )-water produce an increasing thermal conductivity up to 30% in comparison to water base fluid. Eastman and Choi also reported similar enhanced phenomenon for alumina–water, copper oxide–water and copper–oil nanofluids [16]. In the following decades, Yu WH et al. [17] and Eapen et al. [18] demonstrated that several parameters influence the nanofluid thermal conductivity function, *for example*, nanoparticle material, size, shape, volume fraction and spatial distribution, as well as temperature, base fluid type, and pH value. [19–22]. Prasher et al. [23] and Chen et al. [24] studied on aluminum oxide and titanium oxide, respectively, at the temperature range of 20–60 °C. Their result showed that there was not any change to be considered with increasing temperature in relative viscosity. Xie et al. [25] proposed the optimization of the thermal conductivity of nanofluids by various nanoparticles such as  $\text{Al}_2\text{O}_3$  of different sizes,  $\text{SiO}_2$ ,  $\text{Fe}_3\text{O}_4$ ,  $\text{TiO}_2$ , carbon nanotubes, etc. They used base fluids such as deionized water (DW), ethylene glycol (EG), a mixture of DW and EG, etc. Results showed that factors such as the volume fraction of the nanoparticles, nanoparticles sizes, temperature, the base fluid's thermal conductivity, the pre-treatment process, and the additives of the fluids could affect the enhancement of nanofluid thermal conductivity. The results of an investigation on the boundary layer of two-dimensional alumina-water nanofluid showed that the great amount of volume fraction ( $\phi$ ) and the heat capacity ( $C_p$ ) of nanofluid lead to produce more heat energy. It can also be seen that an increase in velocity parameter enhances local skin friction coefficient and reduces local Nusselt number [26]. Another study investigates heat transfer of nanofluid flow within boundary layer generated in the slurry motion (i.e., 36 nm  $\text{Al}_2\text{O}_3$ -water) using numerical approach. The results showed that at smaller amount of volume fraction ( $\phi$ ), the local skin friction coefficient is negligible. Thus, local skin friction coefficient has a corresponding relation with amount of  $\phi$ . Temperature and velocity functions depend on amounts of

internal space dependent heat source parameter. Moreover, smaller amounts of internal space dependent heat source lead to the maximum rate of heat transfer [27].

Artificial neural network (ANN) modeling approaches have been shown to provide good validation tools for measurement of thermal conductivity, particularly in nanotubes applications and experiments [28, 29]. The impact of temperature and volume concentration of zinc oxide–titanium oxide hybrid nanofluid on the thermal conductivity was investigated using ANN [30]. Nasirzadehroshenin et al. developed an experimental and theoretical study to investigate the impact of main variables such as nanofluid volume fraction and temperature on the thermophysical properties and heat transfer of carbon nanotubes–copper oxide–water hybrid nanofluid. This study also predicted the optimum conditions to reach enhanced heat transfer of hybrid nanofluid by using computer-modeling approaches, RSM and ANN [31].

In this present study, synthesized aluminum oxide nanoparticles were incorporated on titanium oxide surface, with thermophysical modification purpose for titanium oxide. Experimental and simulation approaches were applied to explore the impact of main variables such as temperature, nanofluid volume fraction and nanoparticles sizes on thermal conductivity and viscosity of hybrid nanofluid. The relation between variables and optimal results of thermophysical properties was explored using two modeling approaches. Response Surface Methodology-Central Composite Design (RSM-CCD) approach was used to design experiments and optimize the results. Artificial neural network (ANN) was used to predict thermal conductivity and viscosity of hybrid nanofluid accurately. The results demonstrated the utility of these approaches in the study of thermophysical properties of novel hybrid nanofluids and conditions.

## 1.1 Research Questions

The presented study responds some important questions appropriately:

1. How to improve thermal conductivity properties of titanium oxide–water nanofluid?
2. Does improvement obtain in thermophysical properties of hybrid nanofluid compared with water or untreated titanium oxide–water nanofluid?
3. Which main variables affect thermophysical properties of hybrid nanofluid?
4. Is there any possibility to design experiments and predict the optimum results by computer-modeling approaches?
5. In this study, are the modeling approaches such as RSM and ANN useful to predict and determine optimal conditions for hybrid nanofluid's thermophysical properties?



## 2 Materials and Experimental Procedure

Although, titanium oxide ( $\text{TiO}_2$ ) has appropriate mechanical and chemical stability used in different applications, its thermal conductivity increases slightly with an increasing temperature and concentration in comparison with other metal oxides such as aluminum oxide ( $\text{Al}_2\text{O}_3$ ). Thus, thermal conductivity of titanium oxide was modified using  $\text{Al}_2\text{O}_3$  nanoparticles synthesized by sol gel technique.

### 2.1 Synthesizing of $\text{Al}_2\text{O}_3$

Fixed molar ratio of aluminum chloride (Sigma-Aldrich, 98%) was dissolved into ethanol alcohol (Carolina. Co, 95%) and subjected by adding dropwise  $\text{NH}_3$  solution (Scharlau, 25%). Aqueous solution was continuously stirring by a magnetic stirrer for 2 h. (Solution A)

### 2.2 Synthesizing $\text{TiO}_2$

$\text{Ti}(\text{OBU})_4$  (TRC. Co) was dissolved into 10 ml of ethanol alcohol. Solution was continuously stirred by a magnetic stirrer for 2 h at the room temperature to make a homogeneous solution. At the last stage, 5 ml of distilled water was gradually added to the mixture. (Solution B)

### 2.3 Synthesizing Nanocomposite ( $\text{TiO}_2$ -10 wt% $\text{Al}_2\text{O}_3$ )

Solution (A) was added into solution (B) dropwise under the ultrasonication condition for 3 h, finally,  $\text{Al}_2\text{O}_3$  nanoparticles were incorporated on the surface of  $\text{TiO}_2$ . It should be noted that pH must be checked and kept constant at three. Afterward, the synthesized  $\text{TiO}_2$ -10 wt%  $\text{Al}_2\text{O}_3$  nanocomposite was dried in an oven under vacuum condition overnight at  $60^\circ\text{C}$ . The dried gel was calcined at different temperatures 200, 400 and  $500^\circ\text{C}$  for several hours; nanoparticles having various sizes accompanying heat treatments were obtained. Finally, the calcined powders were milled to obtain the fine homogeneous powder.

### 2.4 Characterization of Nanocomposite

The morphology of nanocomposite ( $\text{TiO}_2$ -10 wt%  $\text{Al}_2\text{O}_3$ ) was considered using scanning electron microscopy (SEM, Philips XL30). The structure and size of synthesized nanocomposites were investigated using X-Ray Diffraction (XRD, Rigaku D/MAX-RB diffractometer) with  $\text{CuK}\alpha$ . Radiation  $\lambda = 1.5406$  and an angle of  $2\theta$  between  $20^\circ$  and  $80^\circ$  was applied. The scan was continuously carried out with a current and accelerating voltage of 100 mA and 40 kV, respectively.

## 2.5 Preparation of Hybrid Nanofluid

Preparation process of water-based hybrid nanofluid requires to be followed by the two-step method. Synthesized nanocomposite was gently dispersed into distilled water (as a base fluid). For obtaining such a stable state and preventing of particle agglomeration within the base fluid, 45-min ultrasonication condition is an essential step [32]. Equation (1) is used to estimate the volume fraction of the nanofluid.

The fixed amounts of nanocomposite calculated by Eq. (1) were gently added into water to obtain desired volumetric fractions.

$$\% \text{ volume fraction } \phi = \frac{\left[ \frac{w_{np}}{\rho_{np}} \right]}{\left[ \frac{w_{np}}{\rho_{np}} + \frac{w_w}{\rho_w} \right]} \quad (1)$$

where  $\rho_{np}$  and  $\rho_w$  are the densities of nanoparticles and water, respectively, and  $w_{np}$  and  $w_w$  explain their mass.

## 2.6 Investigation of Thermophysical Properties of Hybrid Nanofluid

The thermal conductivity ( $k$ ) and the dynamic viscosity ( $\mu$ ) of hybrid nanofluids (NFs) were measured using KD2Pro instrument and Brookfield DVII viscometer, respectively, under different conditions of nanofluid volume fraction ranging from 0.0, 0.1, 0.2, 0.25, 0.3, 0.4 to 0.5%, temperature ( $20$  to  $50^\circ\text{C}$ ) and nanoparticles sizes (20, 35 and 50 nm).

There is a lack of a reliable hybrid model consisting all effective essential parameters of temperature, volumetric concentration and size of nanoparticles in an investigation for thermal conductivity. Furthermore, the presented equations for the thermal conductivity of NFs have not been based on nanocomposite or hybrid nanofluids; thus, there was no possibility of matching the data with the equations. In this study, it is thus strived to fit the experimental data based.

## 3 Modeling Approaches (RSM and ANN)

### 3.1 Response Surface Methodology (RSM)

Response surface methodology with a central composite design (CCD) is a powerful computer-modeling approach to design experiments and optimize purposed tasks. In this study, three main variables in three levels including nanofluid volume fraction, temperature and nanoparticle size were introduced to modeling approach as input values, as presented in Table 1. The thermal conductivity and viscosity of hybrid nanofluid were used as outputs. Twenty experimental runs for each coefficient were suggested by

**Table 1** Three main variables in three levels chosen as input introduced to modeling approaches

Input		
Temperature° C	Volume fraction	Nanoparticle size
20	0	20
35	0.25	35
50	0.5	50

RSM-CCD using the Design Expert statistical package. Analysis of variance (ANOVA) contributed to analyze statistically the output data.

Experimental results contributed to the coefficients of the RSM equation lead to a polynomial regression equation, as shown in Eq. 2. The obtained equation expresses the relationships between response data (thermal conductivity or viscosity) and the three used variables. The efficiency of the model was verified by comparison of the predicted values by model and the results of experiments.

$$Y = \beta_0 + \sum \beta_j \cdot X_i + \sum \beta_{jj} \cdot X_j^2 + \sum \beta_{jk} \cdot X_j \cdot X_k \quad (2)$$

where  $Y$ : thermal conductivity and viscosity of the hybrid nanofluid,  $\beta_0$ : intersection point,  $\beta_j$ : linear coefficient,  $\beta_{jj}$ : squared coefficient,  $\beta_{jk}$ : interaction coefficient,  $X_i, X_j^2, X_j, X_k$ : the level of variables.

### 3.2 Artificial Neural Network (ANN)

Artificial neural network with Levenberg–Marquardt Algorithm was applied to predict thermal conductivity and viscosity of hybrid nanofluid. In this study, to utilize an approach with the lowest error, artificial neural network with three layers of an input, a hidden, and an output were designed. The next important step is to determine the optimal neurons' number in different layers. The number of input and output data specifies the neurons' number in the input and output layers, respectively. In order to obtain an optimum number of neurons in the hidden layer, the trial and error technique was utilized. It is monitored that a network with seven neurons in the hidden layer yields the most accurate prediction and the minimum value of mean square error (MSE). Variables such as temperature, volume fraction and size of nanoparticles were introduced as the inputs to the network, and thermal conductivity and viscosity of hybrid nanofluid as outputs.

This process is usually assessed in terms of minimum mean square error (MSE) and maximum R-squared ( $R^2$ ) to show high accuracy of modeling approach performance, as follows in Eqs. (3, 4):

$$MSE = 1/N \sum_{i=1}^N (X_i^{Sim} - X_i^{ANN})^2 \quad (3)$$

$$R^2 = \frac{\sum_{i=1}^N (X_i^{Sim} - \bar{X})^2 - \sum_{i=1}^N (X_i^{Sim} - X_i^{ANN})^2}{\sum_{i=1}^N (X_i^{Sim} - \bar{X})^2} \quad (4)$$

where  $N$  indicates the number of data,  $X_i^{Sim}$  shows the obtained value from simulation or measurement,  $\bar{X}$  the average value, and  $X_i^{ANN}$  represents the value that is calculated by ANN.

## 4 Analysis of Results and discussion

### 4.1 Characterization of Nanocomposite Using XRD

In this study, X-ray diffraction pattern (XRD) provided essential information on the structure and size of synthesized nanocomposite. In addition, it evaluated incorporation of  $Al_2O_3$  nanoparticles on the surface of  $TiO_2$ . XRD patterns of  $TiO_2$ -10% $Al_2O_3$  nanocomposite synthesized at different calcination temperatures are shown in Fig. 1a–c. Diffraction peak for calcination temperature 200 °C or 400 °C was considered at  $2\theta = 25.2^\circ$  corresponding to (101) the crystal face of anatase  $TiO_2$ . Low degree of crystallinity was considered at 200 °C and 400 °C due to their wider diffraction peak and lower intensity. The results also showed that at 200 °C, structure of  $TiO_2$  starts to transform from amorphous to anatase. The diffraction peak in calcination temperature 500 °C, changes to be sharper at  $2\theta = 25.2^\circ$  and other diffraction peaks are observed at  $2\theta = 37.8, 47.9$  and  $62.7^\circ$  associated with (004), (200) and (204). When temperature increases, anatase peaks change to be sharper and more acute; more regular crystal forms were shown. The intensity of the characteristic peaks of  $Al_2O_3$  is weakened or disappeared in the XRD patterns of  $TiO_2$ -10 wt%  $Al_2O_3$ , because of an appropriate merging of  $Al_2O_3$  nanoparticles on the surface of  $TiO_2$  nanoparticles. Diffraction peaks of XRD patterns for nanocomposite are in good agreement with corresponding standard XRD peaks. The average crystal sizes of nanoparticles were calculated using Scherrer–Debye Eq. (5), regarding the width of diffraction peak at  $2\theta = 25.2^\circ$ . The XRD results reveal that the crystal sizes are dependent on calcination temperatures and an increasing temperature result in smaller nanoparticle size, e.g., 50, 35 and 20 nm are obtained at 200, 400 and 500 °C, respectively.

$$D = K\lambda/(\beta\cos\theta) \quad (5)$$

where  $D$  is average size of nanoparticles,  $K$  is shape factor, its value is around 0.94,  $\lambda$  is incident X-ray wavelength,  $\beta$

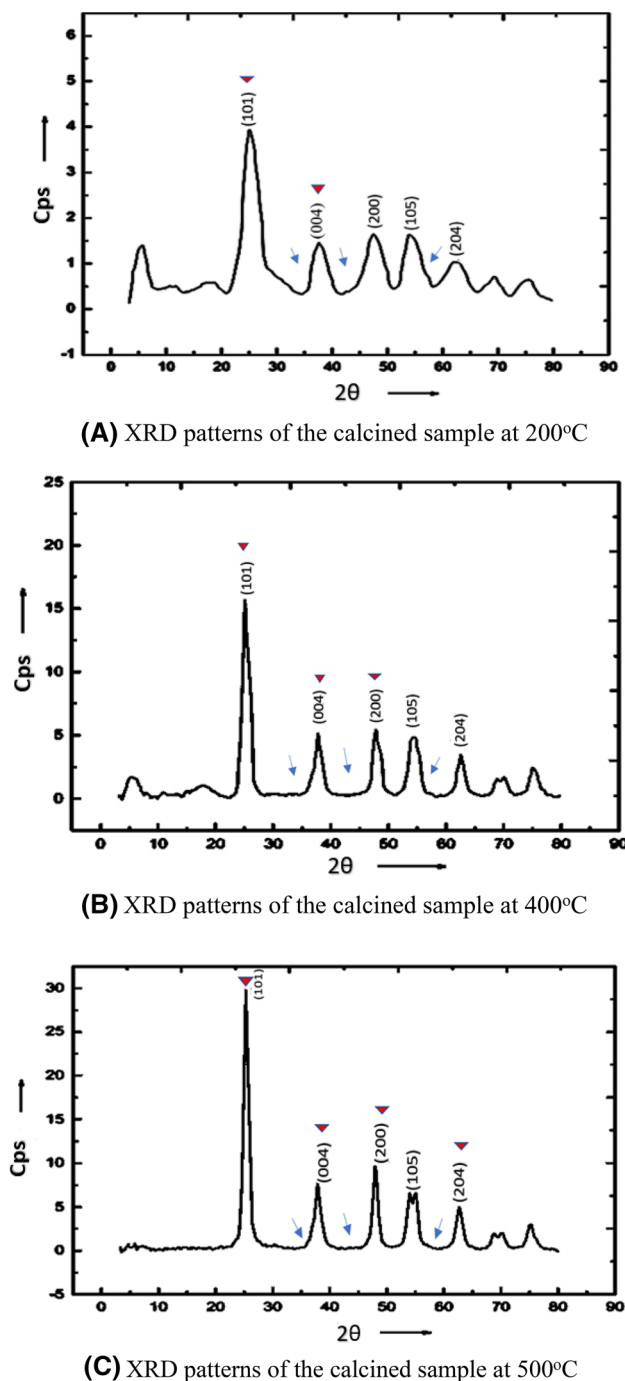


**Fig. 1** Down triangle presents XRD patterns of  $\text{TiO}_2$ -10 wt% $\text{Al}_2\text{O}_3$  and arrows for  $\text{Al}_2\text{O}_3$  picks, at different calcination temperature

is full width at half maximum (FWHM) and  $\theta$  is diffraction angle at maximum intensity peak.

## 4.2 Surface Morphology of Nanocomposite Using SEM

Scanning electron microscope (SEM) images prepared information on morphology of  $\text{TiO}_2$  and  $\text{TiO}_2$ -10 wt% $\text{Al}_2\text{O}_3$

nanocomposites, as shown in Fig. 2. From comparison between  $\text{TiO}_2$  and the  $\text{TiO}_2$ -10 wt%  $\text{Al}_2\text{O}_3$  nanocomposite, it is considered that the surface of  $\text{TiO}_2$  is covered with the layer of materials. Due to decreasing  $\text{TiO}_2$  carrier channels and referring to XRD results, it can be expressed that  $\text{Al}_2\text{O}_3$  has been successfully dispersed on the surface of the titanium oxide, which appeared as white spots on the SEM image consisting small sizes and irregular shapes, as shown by red circles on the image.

## 4.3 Thermal Conductivity and Viscosity Measurements

Thermal conductivity and viscosity of synthesized hybrid nanofluid were experimentally measured. In this case, three main variables affecting thermophysical properties of hybrid nanofluid were involved in measurements; e.g., nanofluid volume fractions (0.0, 0.1, 0.2, 0.25, 0.3, 0.4 and 0.5%), temperature ranged from 20 to 50 °C and nanoparticles sizes including 20, 35 and 50 nm.

As shown in Figs. 3 and 4, both the thermal conductivity and viscosity of hybrid nanofluid have been improved compared with water or untreated titanium oxide–water. In addition, the results showed that three mentioned variables considerably affect the thermophysical properties of hybrid nanofluid; as an increasing volume fraction, reducing nanoparticle size and temperature led to an increasing viscosity while enhanced thermal conductivity was resulted from an increasing nanofluid volume fraction and temperature, and a decreasing nanoparticle size. Increasing nanofluid volume fraction causes more resistance to movement and higher internal viscous shear stresses. The Van der Waals intermolecular forces are weakened with increase in temperature and it leads to more Brownian motion [33, 34]. Improvement of thermal conductivity can be mostly addressed to the nanoparticles stability/dispersion [35], size and shape [36] and Brownian motion.

## 5 The Results of the Modeling Approaches

### 5.1 Statistical Analysis and Model Fitting of RSM

Tables 2 and 3 show the analysis and evaluation of the RSM results using ANOVA test. The  $F$ -value of the model for thermal conductivity and viscosity are 11.66 and 112.74, respectively, which specifies the significance of the model. The significance of each coefficient was examined using  $p$  values. Sentences with  $F < \text{prob value}$  smaller than 0.05 are shown as meaningful sentences.

As shown in Fig. 5, the predicted values are in appropriate agreement with the experimental results as outcomes on the graphs follow the line  $Y=X$ . In ideal case, the predicted

**Fig. 2** SEM image of  $\text{TiO}_2$  and nanocomposite at  $400^\circ\text{C}$  calcination temperature

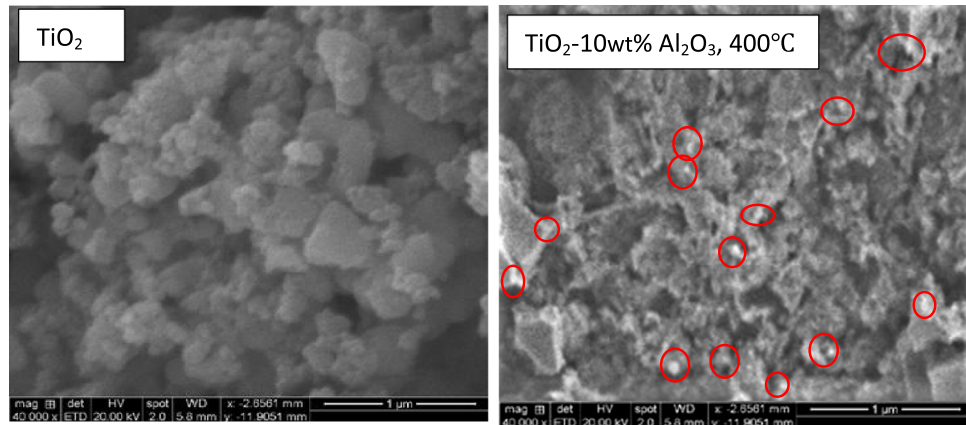
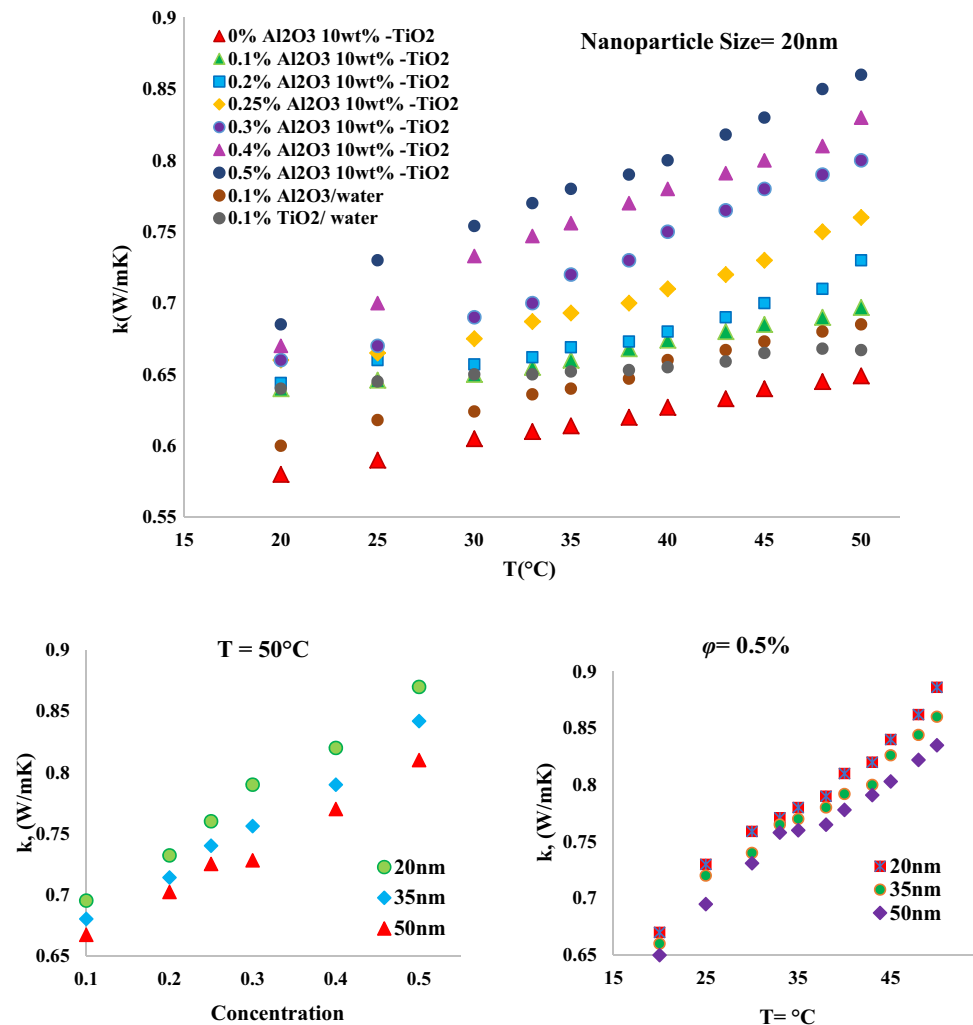


**Fig. 3** Investigation of main variables affecting the thermal conductivity of hybrid nanofluid

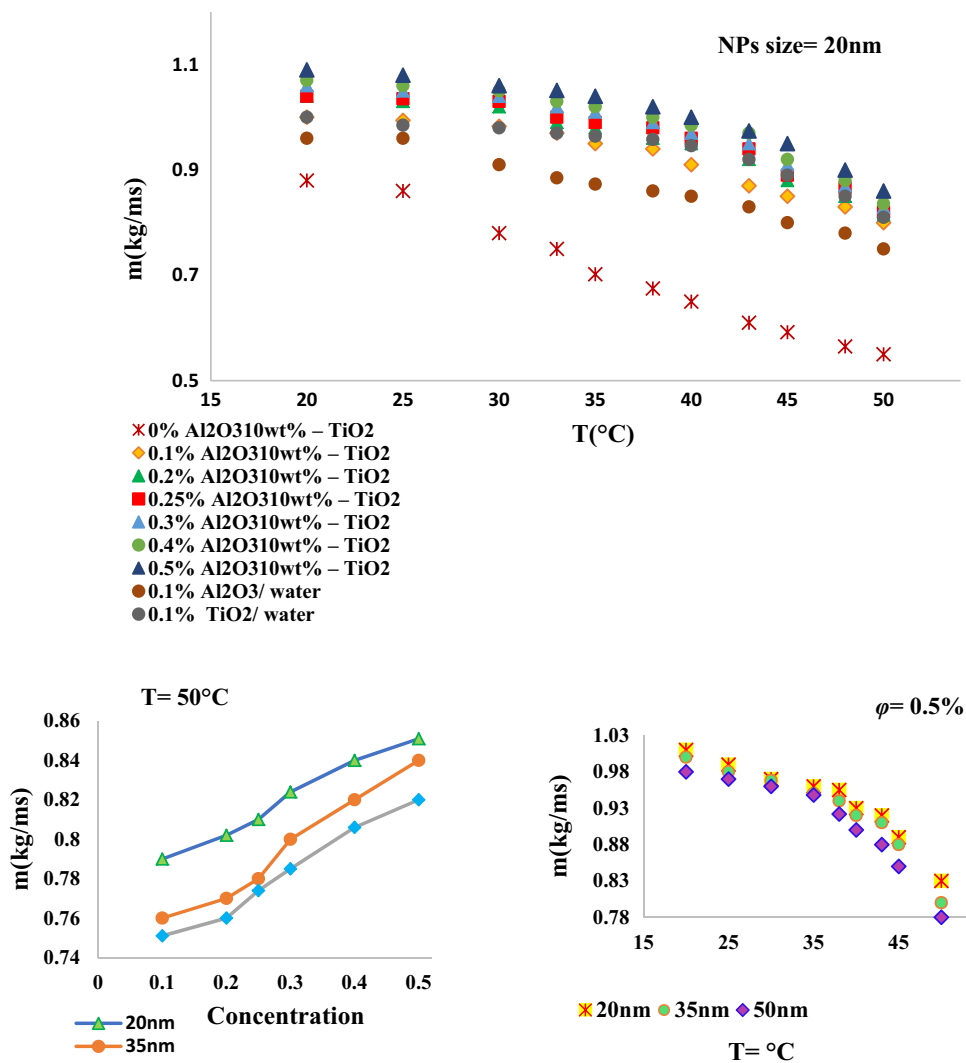


results are completely matched the experimental results when the points on the graphs place on the line  $Y=X$ , which means the modeling approach has been capable to predict purposed values with the highest accuracy. From the normal probability plot of the residuals as shown in Fig. 6, it can be expressed that the residuals scattered around the line follow the normal distribution.

### 5.1.1 Quadratic Formula

After eliminating meaningless sentences, quadratic formula was carried out to predict the thermal conductivity and viscosity of hybrid nanofluid, as presented in Eqs. 6 and 7.

**Fig. 4** Investigation of main variables affecting the viscosity of hybrid nanofluid

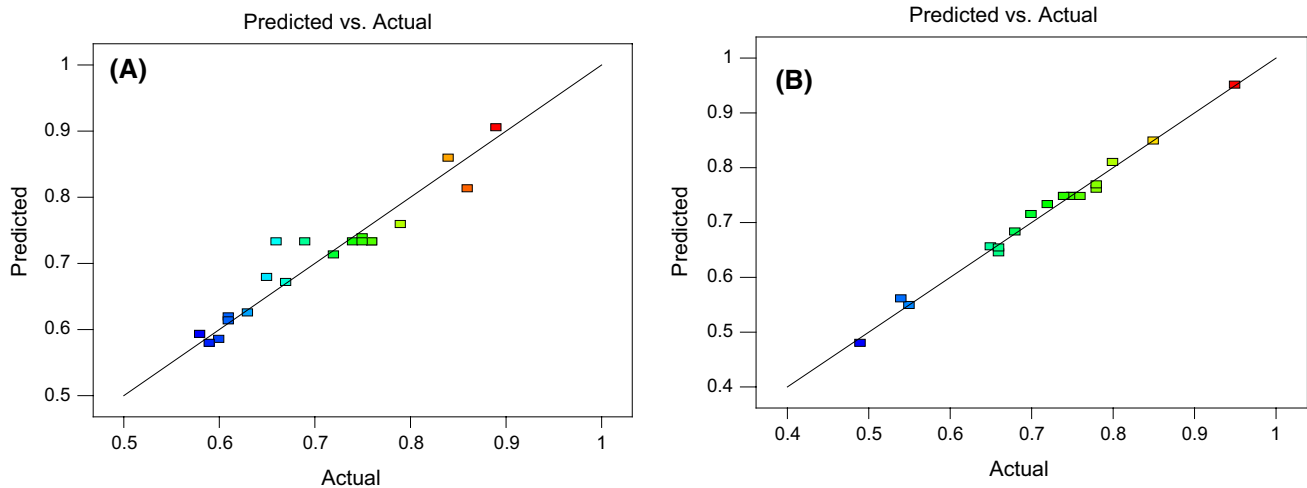


**Table 2** Results of statistical analysis ANOVA test for the viscosity of the hybrid nanofluid

Analysis of variance table [partial sum of squares-type III]						
Source	Sum of squares	df	Mean square	F-value	p value	prob > F
Model	0.21	9	0.024	112.74	<0.0001	Significant
A-Temperature	0.069	1	0.069	326.35	<0.0001	
B-Concentration	0.100	1	0.100	473.73	<0.0001	
C-nanoparticles size	3.240E-003	1	3.240E-003	15.35	0.0029	
AB	1.800E-003	1	1.800E-003	8.53	0.0153	
AC	3.200E-003	1	3.200E-003	15.16	0.0030	
BC	8.450E-003	1	8.450E-003	40.03	<0.0001	
A <sup>2</sup>	9.091E-004	1	9.091E-004	4.31	0.0647	
B <sup>2</sup>	0.021	1	0.021	98.19	<0.0001	
C <sup>2</sup>	2.784E-005	1	2.784E-005	0.13	0.7240	
Residual	2.111E-003	10	2.111E-004			
Lack of fit	1.828E-003	5	3.655E-004	6.45	0.1608	Not significant
Pure error	2.833E-004	5	5.667E-005			
Cor total	0.22	19				

**Table 3** Results of statistical analysis ANOVA test for the thermal conductivity of hybrid NFs

Analysis of variance table [partial sum of squares-type III]						
Source	Sum of squares	df	Mean square	F-value	p value	prob > F
Model	0.15	9	0.017	11.66	0.0003	Significant
A-Temperature	0.045	1	0.045	31.24	0.0002	
B-Concentration	0.069	1	0.069	47.94	< 0.0001	
C-nanoparticles size	1.690E-003	1	1.690E-003	1.18	0.0336	
AB	0.020	1	0.020	13.92	0.0039	
AC	0.000	1	0.000	0.000	1.0000	
BC	8.000E-004	1	8.000E-004	0.56	0.4728	
A <sup>2</sup>	4.778E-004	1	4.778E-004	0.33	0.5769	
B <sup>2</sup>	8.878E-003	1	8.878E-003	6.18	0.0322	
C <sup>2</sup>	1.278E-004	1	1.278E-004	0.089	0.7716	
Residual	0.014	10	1.437E-003			
Lack of fit	5.638E-003	5	1.128E-003	0.65	0.6786	Not significant
Pure error	8.733E-003	5	1.747E-003			
Cor total	0.17	19				

**Fig. 5** Comparison of the predicted data by RSM and experimental results of thermal conductivity results (a) and Viscosity of hybrid nanofluid (b)

$$\begin{aligned}
 \text{Thermal conductivity} = & 0.59489 \\
 & - 2.96768E003 \text{ Temperature} \\
 & + 0.41321 \text{ Concentration} + 1.92121E \\
 & - 003 \text{ nanoparticles size} \\
 & + 0.013333 \text{ Temperature Concentration} + 3.76989E \\
 & - 019 \text{ Temperature nanoparticles size} - 2.66667E \\
 & - 003 \text{ Concentration nanoparticles size} + 5.85859E \\
 & - 005 \text{ Temperature}^2 - 0.90909 \text{ Concentration}^2 \\
 & - 3.03030E - 005 \text{ nano particles size}^2
 \end{aligned}$$

(6)

$$\begin{aligned}
 \text{Viscosity} = & 0.91094 - 0.013301 \text{ Temperature} \\
 & + 1.53788 \text{ Concentration} - 3.13434E \\
 & - 003 \text{ nano particles size} - 4.00000E \\
 & - 003 \text{ Temperature Concentration} + 8.88889E \\
 & - 005 \text{ Temperature nanoparticles size} \\
 & - 8.66667E - 003 \text{ Concentration nanoparticles size} \\
 & + 8.08081E - 005 \text{ Temperature}^2 \\
 & - 1.38909 \text{ Concentration}^2 \\
 & + 1.41414E - 005 \text{ nano particles size}^2
 \end{aligned}$$

(7)



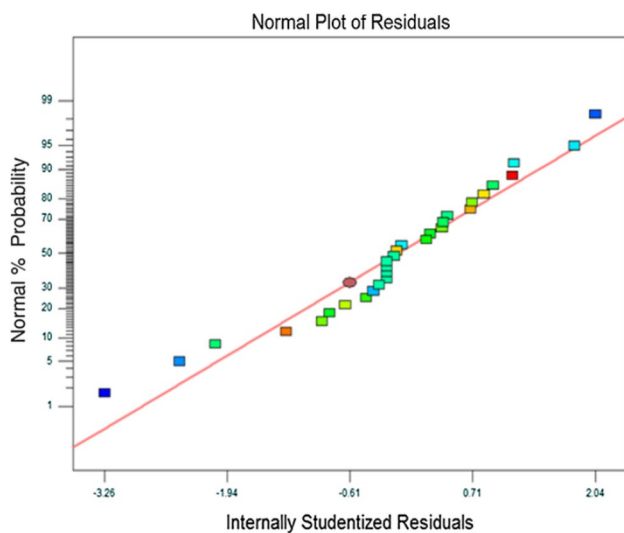


**Fig. 6** Investigation of normal probability of internally studentized residuals

### 5.1.2 RSM Graphical Analysis

RSM three-dimensional (3D) surface and two-dimensional (2D) contour simulation plots of variables affecting the thermal conductivity and viscosity are shown in Figs. 7 and 8. While each plot illustrates the involved variables with interactions, other factors are assumed constant. As Figs. 7 and 8 show, all variables including temperature, nanofluid volume fraction and nanoparticle size could significantly affect the thermal conductivity and viscosity of hybrid nanofluid.

### 5.1.3 Validation of the RSM and Optimization

To validate response surface methodology performance, other sets of the experiments were accomplished using Design Expert software. Strong correlation between the experimental and the predicted values by RSM demonstrated the highest accuracy of approach for modeling the tasks. As shown in Figs. 9 and 10, under the optimal conditions, e.g., 0.5% volume fraction, 20 nm nanoparticle size and temperature 50 °C, optimal thermal conductivity could be estimated 0.89 W/m.K. Optimum viscosity was obtained at 0.95 mPa.s when volume fraction, nanoparticles size and temperature were optimized to 0.5%, 20 nm and 20 °C, respectively. Desirability values for the optimized points of thermal conductivity and viscosity of hybrid nanofluid are equal to one that mean a highly successful optimization.

## 5.2 Artificial Neural Network (ANN)

Artificial neural network (ANN) was developed for theoretical analysis of thermophysical properties of hybrid nanofluids. The neural network arranges data in terms of weights

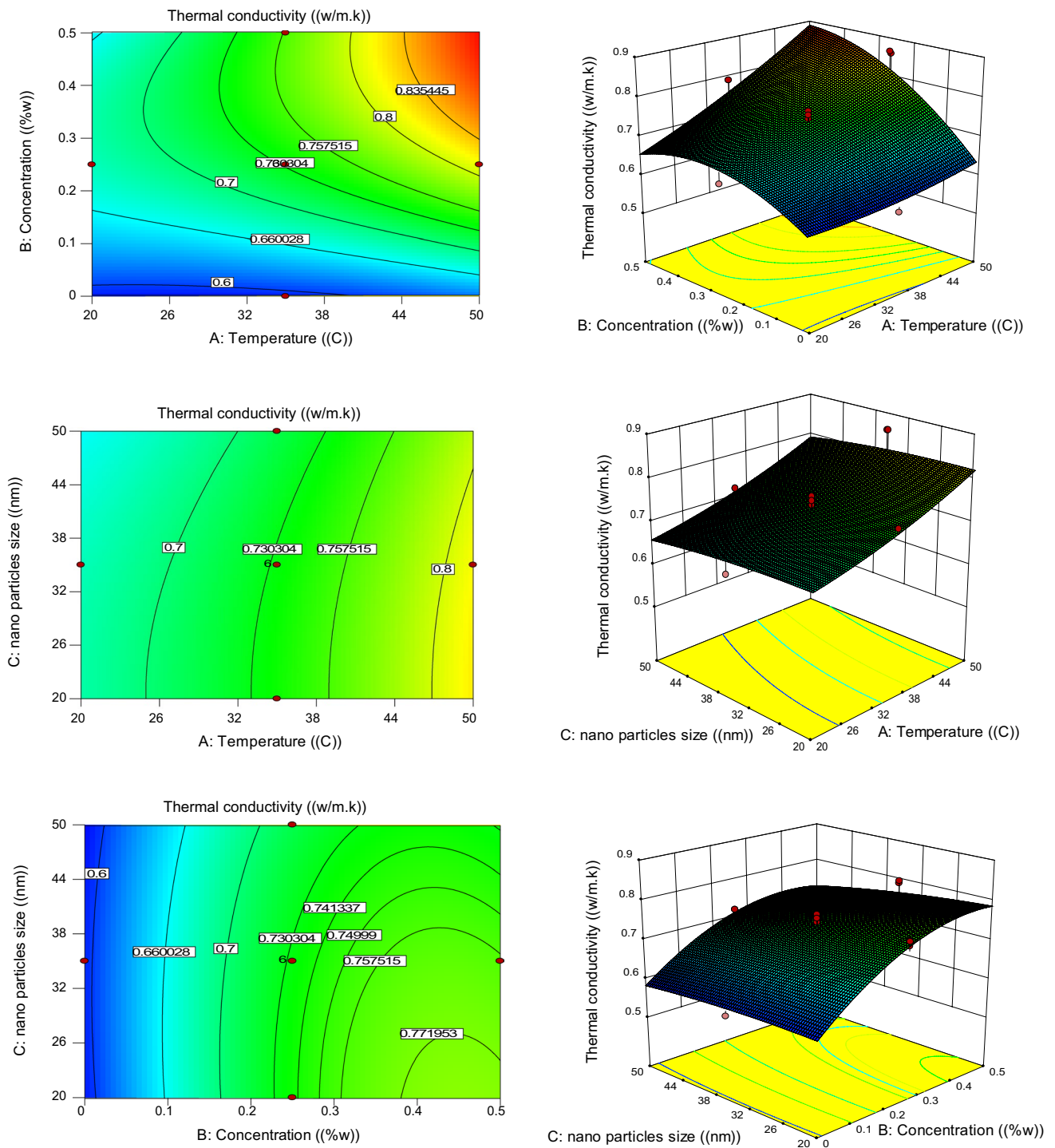
and bias values divided into three data layer including training, validation, and testing sets. Training sets can minimize the error function of the networks. Additionally, validation sets contribute to monitoring of the error function and select the network with the lowest error value. In this study, the total number of data was 62 divided into 58% training, 13% validation and 29% testing data. Three variables including temperature, volume fraction and nanoparticles sizes were introduced to the neural network as inputs and, thermal conductivity and viscosity of hybrid nanofluid as outputs. The best ANN model was chosen based on its predictive accuracy for estimation of thermophysical properties; efficiency of different ANN approaches was compared by the trial and error technique. The best one was selected with seven neurons in hidden layer as it is monitored from Table 4; demonstrated the most accurate approach with the minimum mean square error (MSE) for modeling the considered task.

Figure 11 shows the error between experimental findings and predicted outcomes for measurements of hybrid nanofluid's viscosity. In the error diagram, results plotted for the total data (62 data) indicate an appropriate match between the both groups of data.

Predicted values by ANN for hybrid nanofluid's viscosity were graphically compared with the experimental results, as shown in Fig. 12. The horizontal axis ( $X$ ) indicates the experimental results, and the vertical axis ( $Y$ ) illustrates the predicted data. Ideally, predicted outcomes completely match the experimental results when the prediction error of the neural network is zero and the correlation coefficient ( $R$ ) is close to one; in this case, thus, the points place on the line  $Y=X$ , which means the ANN has been capable to estimate purposed values with the highest precision.

The mean squared error (MSE) is plotted for the training, validation, and test data as shown in Fig. 13, and horizontal axis shows the number of algorithm repetitions in the network training process. The predicted values by ANN are continuously changed to reach the best model based on its predictive accuracy for estimation of thermophysical properties, and the most efficient one is selected with the lowest error. As the graph illustrates, training error is a large amount at the beginning of the trend, and the error value decreases as repetition moves forward. Validation error reaches its minimum amount at epoch 16, and it subsequently moves upward by the end of the trend; thus, the algorithm repetitions has stopped at repeat 22, and the least validation error appeared at epoch 16 is chosen as the response.

Figure 14 graphically illustrates the comparison of the predicted values by ANN and experimental results for thermal conductivity of hybrid nanofluid. The strong correlation between predicted and experimental results ( $R$ -squared of 0.9439 and minimum MSE error of 0.00053) shows highly accurate performance of modeling approach, and the placement of both experimental and predicted results



**Fig. 7** 2D and 3D simulation plots of interactions between variables affecting the thermal conductivity of hybrid nanofluid

on the vicinity of  $X = Y$  line demonstrates high precision of the approach for modeling the considered task. Figure 15 shows highly accurate performance for purposed task by the computer-modeling approach, as it indicates the closeness of model-predicted values and experimental results of thermal conductivity.

## 6 Conclusion

The presented study explored experimentally and theoretically the impact of variables such as temperature, nano-fluid volume fraction and nanoparticle size on thermal

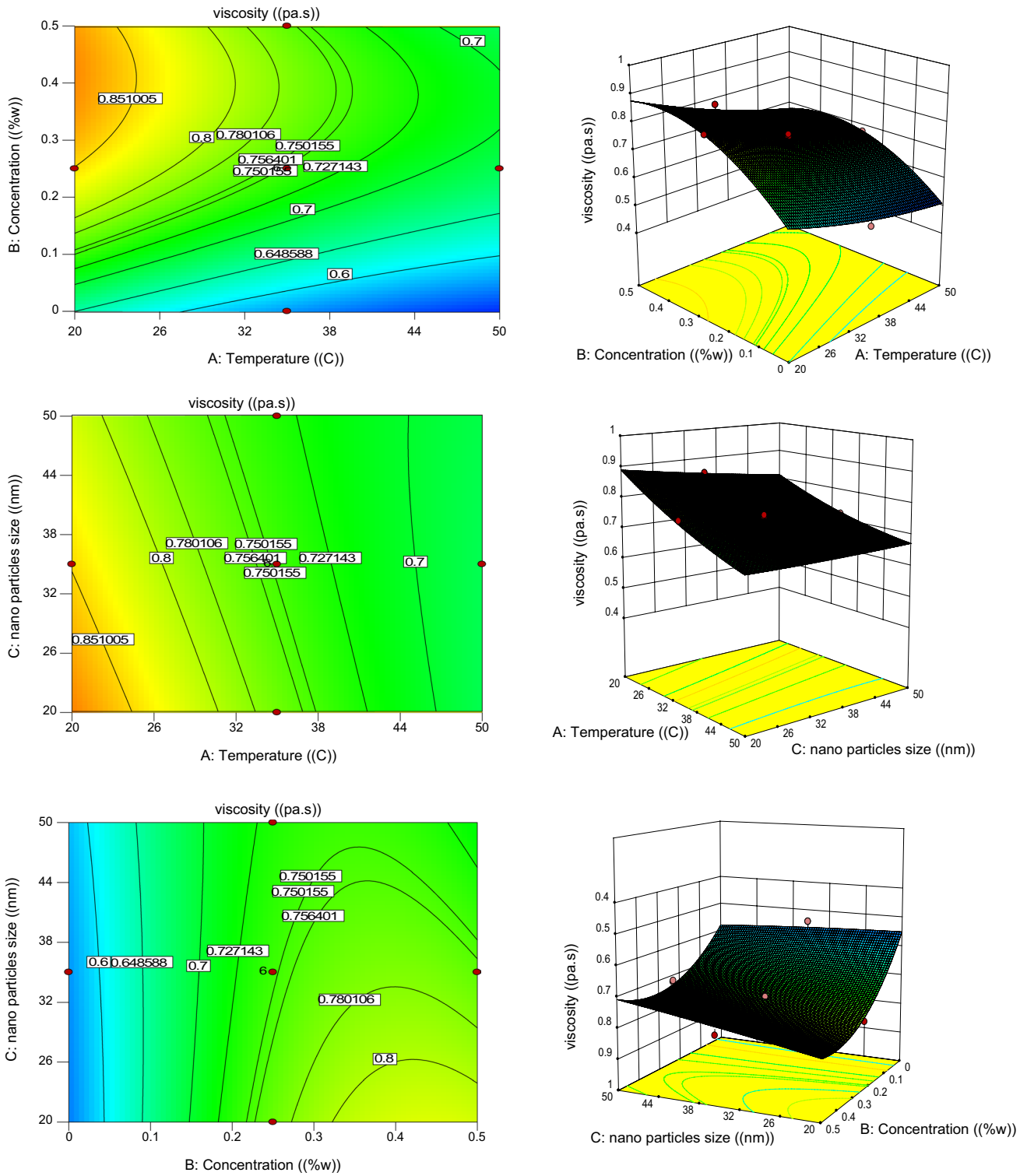


**Fig. 8** 2D and 3D simulation plots of interactions between variables affecting the viscosity of hybrid nanofluid

conductivity and viscosity of hybrid nanofluid. The results show that an increasing temperature and nanofluid volume fraction and a reduction in nanoparticle size result

in an increased thermal conductivity. An enhanced nanofluid viscosity was also observed with increasing volume fraction of nanofluid and a reduction in temperature and

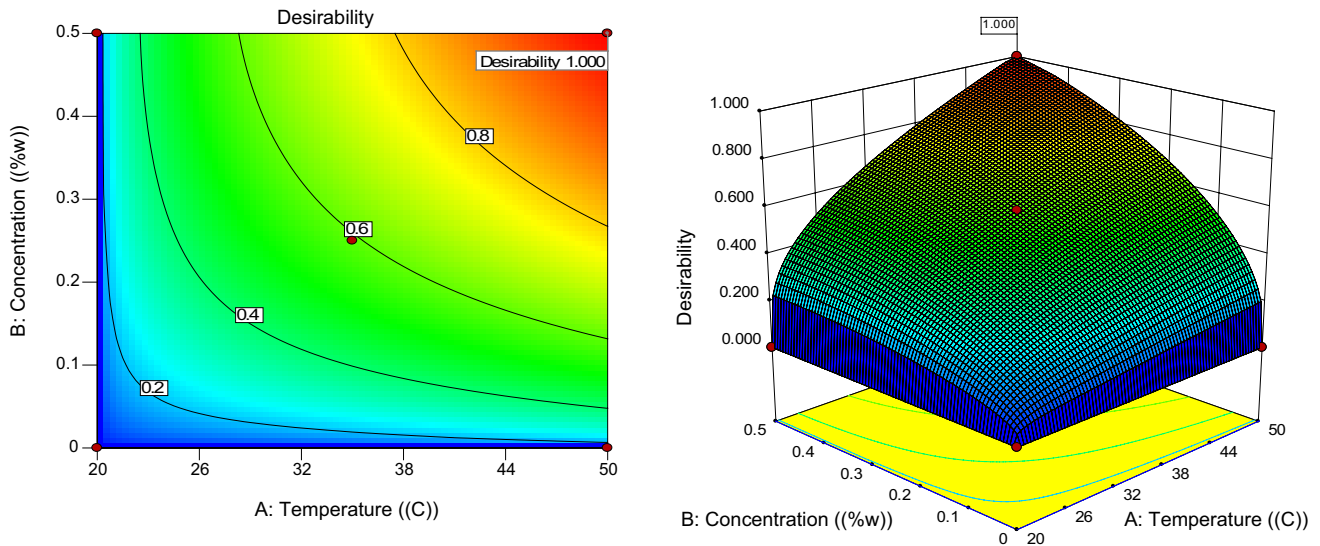


**Fig. 9** Optimum conditions and desirability for the thermal conductivity of hybrid nanofluid

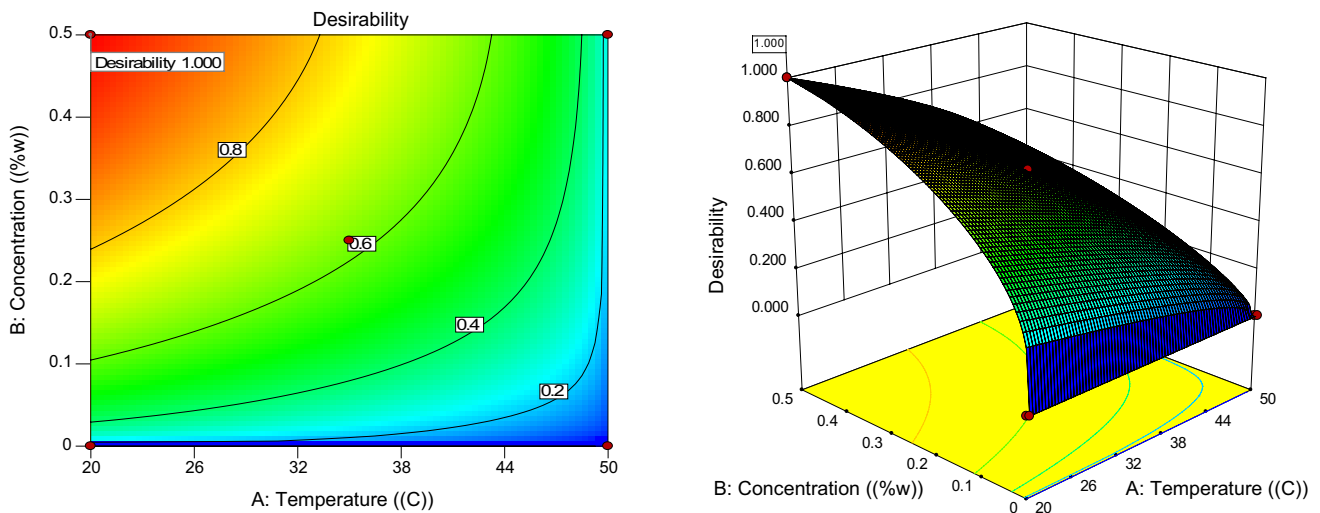


**Fig. 10** Optimum conditions and the desirability for the viscosity of hybrid nanofluid

**Table 4** ANN results of investigation the neuron numbers using various configurations

Network number	Neurons in hidden layer	Correlation coefficient	MSE
1	4	0.793	0.095
2	5	0.816	0.088
3	6	0.83	0.051
4	7	0.86	0.017
5	8	0.75	0.036
6	9	0.71	0.047
7	11	0.81	0.057

nanoparticle size. The experimental results indicate a significant enhancement of thermophysical properties of prepared hybrid nanofluids compared with water or untreated titanium oxide–water.

The characterization of synthesized nanocomposite ( $\text{TiO}_2$ -10 wt%  $\text{Al}_2\text{O}_3$ ) showed the successful incorporation of aluminum oxide on the surface of titanium oxide ( $\text{TiO}_2$ - $\text{Al}_2\text{O}_3$ ), and different calcination temperature led to obtain various sizes of nanoparticles (20, 25 and 50 nm).

Two computer modeling approaches (ANN and RSM) developed a theoretical study to explore the impact of different conditions of temperature, volume fraction and

**Fig. 11** Error between predicted data by neural network and experiment results

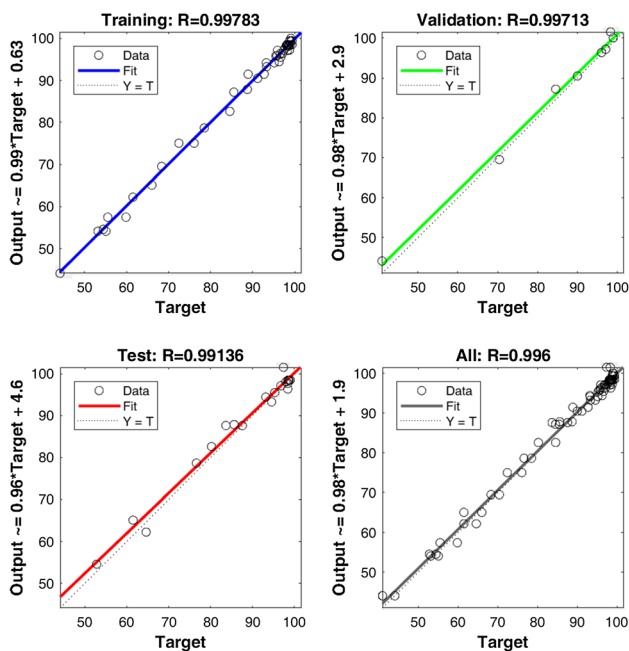
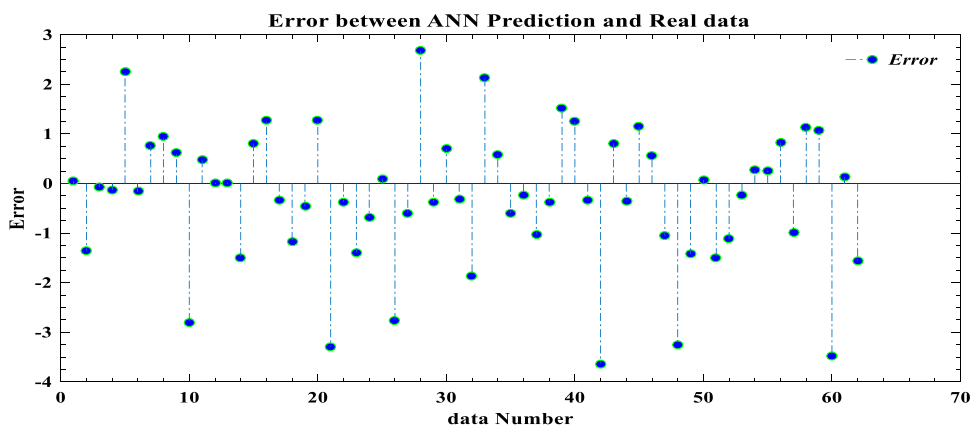


**Fig. 12** The comparative study of ANN predicted and experimental results for hybrid nanofluid viscosity

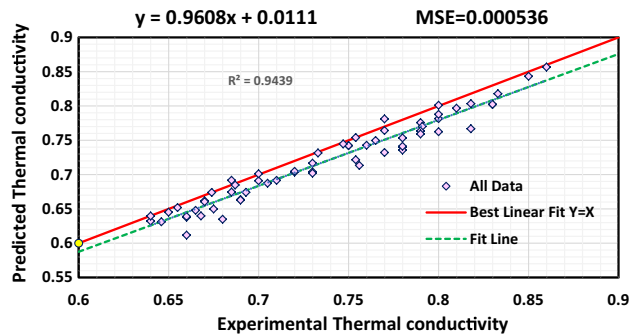


**Fig. 14** Scatter diagram for thermal conductivity based on ANN

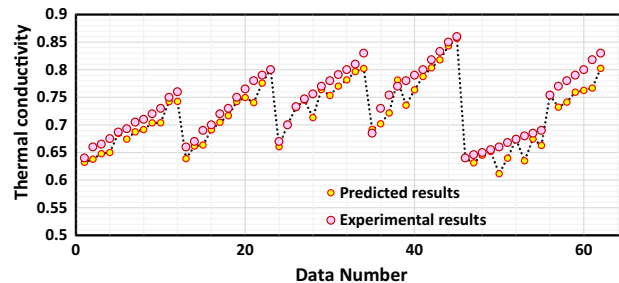


**Fig. 15** Comparison of ANN and experimental results of nanofluid thermal conductivity

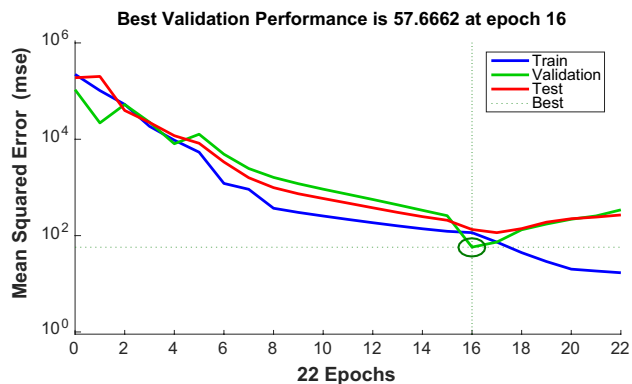


**Fig. 13** Comparison the mean squared error for the training, validation, and test data

nanoparticle size on hybrid nanofluid’s thermophysical properties. In this study, optimal thermal conductivity and viscosity for hybrid nanofluid were predicted to be 0.89 W/m.K and 0.95 mPa.s, respectively. Desirability values for the optimized points of thermal conductivity and viscosity are equal to one that means a successful optimization. The close relationship between experimental results and model-estimated values indicates that ANN and RSM approaches accurately predicted the impact of these modifications on thermophysical properties, demonstrated the most accurate approaches for modeling the considered task and confirmed the experimental outcomes.

## References

- Hussein, A.M.; Bakar, R.A.; Kadrigama, K.; Sharma, K.V.: Experimental measurement of nanofluids thermal properties. *Int. J. Automotive Mech. Eng.* (2013). <https://doi.org/10.15282/ijame.7.2012.5.0070>
- Yu, W.; France, D.M.; Routbort, J.L.; Choi, S.U.S.: Review and comparison of nanofluid thermal conductivity and heat transfer enhancements. *Heat Transfer Eng.* **29**, 432–460 (2008)
- Tyler, T.; Shenderova, O.; Cunningham, G.; Walsh, J.; Drobnik, J.; McGuire, G.: Thermal transport properties of diamond-based nanofluids and nanocomposites. *Diam. Relat. Mater.* **15**, 2078–2081 (2006)
- Das, S.K.; Choi, S.U.S.; Patel, H.E.: Heat transfer in nanofluids, a review. *Heat Transfer Eng.* **27**(10), 3–19 (2006)
- Liu, M.S.; Lin, M.C.C.; Huang, I.T.; Wang, C.C.: Enhancement of thermal conductivity with carbon nanotube for nanofluids. *Int. Commun. Heat Mass Transfer* **32**, 1202–1210 (2005)
- Choi, S.U.S.; Zhang, Z.G.; Keblinski, P.; Nalwa, H.S. (eds.): *Nanofluids*, in encyclopedia of nanoscience and nanotechnology, vol. 6, pp. 737–757. American Scientific Publishers, Los Angeles (2004)
- Murshed, S.M.S.; Tan, S.H.; Nguyen, N.T.: Temperature dependence of interfacial properties and viscosity of nanofluids for droplet-based microfluidics. *J. Phys. D Appl. Phys.* **41**(085502), 1–5 (2008)
- Wong, K.V.; Kurma, T.: Transport properties of alumina nanofluids. *Nanotechnology* **19**(345702), 8 (2008)
- Wong, K.V.; Bonn, B.; Vu, S.; Samed, S.: Study of nanofluid natural convection phenomena in rectangular enclosures. In: *Proceedings of IMECE 2007*, Nov. 2007, Seattle
- Minkowycz, W.; et al.: *Nanoparticle Heat Transfer and Fluid Flow*. CRC Press, Boca Raton (2013)
- Das, S.K.; Stephen, S.U.; Choi, W.Yu.; Pradeep, T.: *Nanofluids Science and Technology*, p. 397. Wiley, New Jersey (2007)
- Kakaç, S.; Pramuanjaroenkij, A.: Review of convective heat transfer enhancement with nanofluids. *Int. J. Heat Mass Transf.* (2009). <https://doi.org/10.1016/j.ijheatmasstransfer.2009.02.006>
- Sundar, L.S.; Sharma, K.V.; Singh, Manoj K.; Sousa, A.C.M.: Hybrid nanofluids preparation, thermal properties, heat transfer and friction factor—a review. *Renew. Sustain. Energy Rev.* **68**(P1), 185–198 (2017)
- Choi, S.U.S.: Nanofluids: from vision to reality through research. *J. Heat Transfer* **131**(3), 9 (2009)
- Masuda, H.; Ebata, A.; Teramea, K.; Hishinuma, N.: Alteration of thermal conductivity and viscosity of liquid by dispersing ultra-fine particles. *Netsu Bussei* **4**, 227–233 (1993)
- Eastman, J.A.; Choi, U.S.; Li, S.; Thompson, L. J.; Lee, S.: Enhanced thermal conductivity through the development of nanofluids. In: Komarneni, S., Parker, J. C., Wollenberger, H. J., (eds.) *Nanophase and Nanocomposite Materials II*. pp. 3–11. Materials Research Society, Pittsburg (1997)
- Yu, W.H.; France, D.M.; Routbort, J.L.; Choi, S.U.S.: Review and comparison of nanofluid thermal conductivity and heat transfer enhancements. *Heat Transfer Eng.* **29**, 432–460 (2009)
- Eapen, J.; Rusconi, R.; Piazza, R.; Yip, S.: The classical nature of thermal conduction in nanofluids. *J. Heat Transfer* **132**, 102402-1–102402-14 (2010)
- Rusconi, R.; Rodari, E.; Piazza, R.: Optical measurements of the thermal properties of nanofluids. *Appl. Phys. Lett.* **89**, 2619161–2619163 (2006)
- Putnam, S.A.; Cahill, D.G.; Braun, P.V.: Thermal conductivity of nanoparticle suspensions. *J. Appl. Phys.* **99**, 084308-1–084308-6 (2006)
- Venerus, D.C.; Kabadi, M.S.; Lee, S.; Perez-Luna, V.: Study of thermal transport in nanoparticle suspensions using forced Rayleigh scattering. *J. Appl. Phys.* **100**, 0943101–0943105 (2006)
- Buongiorno, J.; Venerus, D.C.; Prabhat, N.: A benchmark study on the thermal conductivity of nanofluids. *J. Appl. Phys.* **106**, 094312-1–094312-14 (2009)
- Prasher, R.: Measurements of nanofluid viscosity and its implications for thermal applications. *Appl. Phys. Lett.* **89**(13), 133108 (2006)
- Chen, H.; Yulong, D.; Chunqing, T.: Rheological behaviour of nanofluids. *New J. Phys.* **9**(10), 367 (2007)
- Xie, H.; Yu, W.; Li, Y.; Chen, L.: Discussion on the thermal conductivity enhancement of nanofluids. *Nanoscale Res. Lett.* **6**, 1–24 (2011)
- Animasaun, I.L.: 47nm Alumina–water nanofluid flow within boundary layer formed on upper horizontal surface of paraboloid of revolution in the presence of quartic autocatalysis chemical reaction. *Alex. Eng. J.* **55**, 2375–2389 (2016)
- Animasaun, I.L.; Sandeep, N.: Buoyancy induced model for the flow of 36 nm alumina–water nanofluid along upper horizontal surface of a paraboloid of revolution with variable thermal conductivity and viscosity. *Powder Technol.* (2016). <https://doi.org/10.1016/j.powtec.2016.07.02>
- Hemmat Esfe, M.; Esfandeh, S.; Saedodin, S.; Rostamian, H.: Experimental evaluation, sensitivity analysis and ANN modeling of thermal conductivity of ZnO-MWCNT/EG-water hybrid nanofluid for engineering applications. *Appl. Therm. Eng.* **125**(2017), 673–685 (2017). <https://doi.org/10.1016/J.APPLTHERMALENG.2017.06.077>
- Moradikazerouni, A.; Hajizadeh, A.; Safaei, M.R.; Afrand, M.; Yarmand, H.; Zulkifli, N.W.B.M.: Assessment of thermal conductivity enhancement of nano-antifreeze containing single-walled carbon nanotubes: optimal artificial neural network and curve-fitting. *Phys. A Stat. Mech. Appl.* **521**(2019), 138–145 (2019). <https://doi.org/10.1016/j.physa.2019.01.051>
- Yarmand, H.; Afrand, M.; Safaei, M.R.; Zulkifli, N.W.B.M.; Qi, C.; Hajizadeh, A.: Evaluating the effect of temperature and concentration on the thermal conductivity of ZnO-TiO<sub>2</sub>/EG hybrid nanofluid using artificial neural network and curve fitting on experimental data. *Phys. A Stat. Mech. Appl.* **519**(2018), 209–216 (2018). <https://doi.org/10.1016/j.physa.2018.12.010>
- Nasirzadehroshenin, F.; Maddah, H.; Sakhaeinia, H.; Pourmoza-fari, A.: Investigation of exergy of double-pipe Heat exchanger using synthesized hybrid nanofluid developed by modeling. *Int. J. Thermophys.* **40**, 87 (2019). <https://doi.org/10.1007/s10765-019-2551-z>
- Manasrah, A.D.; Al-Mubaiyedh, U.A.; Lau, T.; Ben Mansour, R.; Al-Marri, M.J.; Almanassra, I.W.; Abdala, A.; Atieh, M.A.: *Appl. Therm. Eng.* **107**, 1008–1018 (2016)
- Chandraprabu, V.; Sankaranarayanan, G.; Iniyar, S.; Suresh, S.: Heat transfer enhancement characteristics of Al<sub>2</sub>O<sub>3</sub>/Water and CuO/Water nanofluids in a tube in tube condenser fitted with an air conditioning system—an experimental comparison. *J. Therm. Sci. Eng. Appl.* **6**(041004), 1–5 (2014)
- Venkateshan, T.; Eswaramoorthi, M.: A review on performance of heat exchangers with different configurations. *Int. J. Res. Appl. Sci. Eng. Technol.* **3**, 2321–9653 (2015)
- Jung, J.-Y.; Cho, C.; Lee, W.H.; Kang, Y.T.: *Int. J. Heat Mass Transfer* **54**, 1728–1733 (2011)
- Eastman, J.A.; Choi, S.; Li, S.; Yu, W.; Thompson, L.: *Appl. Phys. Lett.* **78**, 718–720 (2001)

